Estimates of two-point, broadband temporal coherence using a *z*-transform technique

C. Feuillade[a] and W. A. Kinney
Naval Ocean Research and Development Activity, NSTL, Mississippi 39529-5004

(Received 1 September 1987; accepted for publication 18 May 1988)

Values of broadband coherence versus time delay are presented for two horizontally separated receivers in water overlying a rigid bottom. These values are given for different source azimuth angles (from broadside to endfire) and for (a) surface-bottom (SB) paths, (b) bottom-surface (BS) paths, and (c) a combination of SB and bottom-reflected (B) paths. The acoustic wavelength band considered is the passband from 0.2–1.0 m. The water depth and range are both 5 km. The source and receivers are all at 200 m depth, with the receivers separated by 25 m. The ocean bottom is assumed to be rigid and flat. Scattering from the ocean surface is modeled using the time-domain, facet-ensemble method [H. Medwin, J. Acoust. Soc. Am. **69**, 1060–1064 (1981); C. S. Clay and W. A. Kinney, J. Acoust. Soc. Am. **83**, 2126–2133 (1988)] applied to a long-crested wave model of the ocean surface using actual wave-height measurements with an rms value of 1 m. A *z*-transform algorithm (suggested by C. S. Clay) is used to perform broadband filtering and to compute coherence. Results demonstrate how signals that arrive endfire via SB paths possess greater coherence (with values near 0.8) than signals that arrive via BS paths (values near 0). This is because the SB path involves scattering off areas on the ocean surface that are close together and physically similar.

PACS numbers: 43.30.Hw, 43.20.Fn

INTRODUCTION

Two horizontally separated receivers can be used to locate a submerged sound source by correlating the received signals. The signal arriving at each receiver does so via multiple paths (e.g., B, SB, and BS, see Fig. 1). The degree to which the signals at the two receivers are correlated depends in large part on the physical features of the boundaries at the ocean surface and the ocean bottom.

This article presents a technique for estimating the broadband loss in coherence between two received signals due to ocean surface roughness alone. The technique utilizes the facet-ensemble method for modeling rough surface scattering.[1,2] The acoustic wavelength band considered is from 0.2–1.0 m. In this problem, the ocean bottom is assumed to be flat and rigid. Both the depth of the water column and the range between the source and receivers are 5 km (see Fig. 1). The depths of the source and receivers are all 200 m (with one notable exception to be discussed).

The problem of estimating the coherence loss at two receivers due to rough surface scattering has received previous attention in the literature. Parkins' formalism[3] describes the space and time variation of cw acoustic signals reradiated from a time-varying ocean surface in terms of local reflection from a series of facets (i.e., the "broken-mirror" approach). Diffraction effects at the facets are neglected, and the problem of broadband coherence loss is not addressed. McDonald *et al.*[4] have used the Fresnel corrected Kirchhoff approximation to compute the interfrequency correlation function of scattered signals. Their work relates frequency shift, time lag, and spatial separation of the receivers. Again, the fully broadband correlation problem in the time domain is not considered. Brill and his co-workers[5,6] have also used a broken-mirror approximation to calculate time, frequency, and angle spreads of acoustic signals reflecting from a fixed rough boundary.

The facet-ensemble method was developed to overcome inaccuracies in other theories with regard to diffraction, in particular, and reflection, in general. The two physical processes are different and cannot be treated in time-separated form with the same analytical formalism. Rough-surface diffraction contributions are treated in the method by using the exact three-dimensional solution for diffraction from a rigid (or pressure release) wedge or trough.[1] The reflected contributions from facets (wedge halves) that are specularly oriented are treated based on a new interpretation of the Rubinowicz formulation.[2] In its present form, the facet-ensemble method calculates the three-dimensional scattered field for surfaces possessing features for which height varies in only one direction (i.e., long-crested features). The method has been shown to be accurate and robust in comparisons with experimental data and is particularly well suited to the problem being addressed in this article.[1,7,8] Currently, it is being modified to handle three-dimensional surfaces approximated using triangular facets.

The method can provide both frequency-domain and time-domain-impulse solutions. In this problem, a surface-scattered impulse response is computed for each receiver and then convolved (using a *z*-transform technique) with a time-domain broadband filter. The broadband-filtered sig-

[a] Employee of Syntek Engineering Inc., 2101 E. Jefferson St., Rockville, MD 20852.

 0001-4966/88/091030-07$00.80

nal at one receiver is then correlated in time (again using z-transforms) with the filtered signal at the other receiver. The correlation is averaged over different "looks" at the model surface. The surface is deterministically modeled in cross section over a spatial interval that is large compared to the ensonified region of interest. In the problem discussed here, the surface cross section (a segment of which is shown in Fig. 4) is taken from actual temporal waveheight (wave-rider buoy) measurements with a root-mean-square (rms) value of approximately 1 m.[9] The spatial waveheight values are derived assuming a mean wave speed of 7.7 ms^{-1}. The facet-ensemble method uses a Monte Carlo approach in that it averages over different discrete looks at a deterministic representation of the surface.

Section I of this article contains a discussion of the specific z-transform techniques used to calculate the broadband correlation versus time for two receivers. Section II provides results for the case of two horizontally separated receivers in the presence of a rough ocean surface and a flat rigid ocean bottom. Results are provided for individual cases involving (a) SB paths alone, (b) BS paths alone, and (c) a superposition of SB and B paths. The results include correlation as a function of azimuth (from broadside to endfire) and relative depth of the two receivers. An explanation is given as to why the correlation is better in the case of SB paths than it is in the case of BS paths. Section III provides a set of conclusions derived from the results.

I. THEORY

A z-transform technique is used to perform the numerical correlation and convolution of the time-dependent signals that will be discussed here. Since the z-transform method is very well established in the literature,[10] only a brief pertinent outline of it will be given.

Assume that an extended, time-dependent signal $P(t)$, arriving at receiver A in Fig. 1, may be approximated by the series

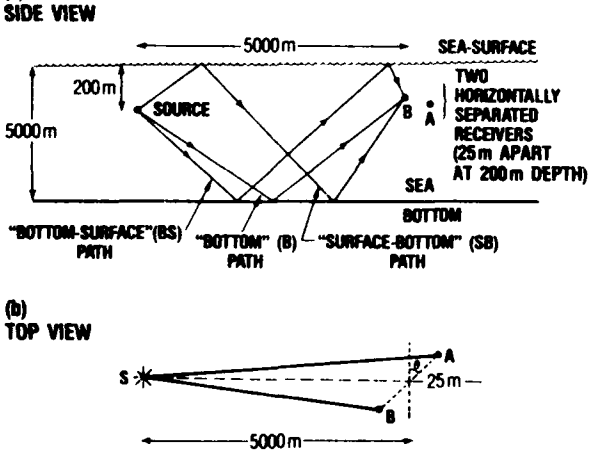

FIG. 1. (a) Schematic diagram showing the side view of the geometrical arrangement of the submerged source and receivers (A and B at the same depth and separated by 25 m) together with the three types of acoustic ray paths (B, SB, BS) (not to scale). (b) Top view of the geometrical layout (with azimuthal rotation).

$$P_a(z) = \sum_n a_n z^n \quad (n = 0,1,2,3,\ldots)\,, \tag{1}$$

where

$$z = e^{i\omega\Delta t}\,, \tag{2}$$

where ω is 2π times the sampling frequency and Δt is the sampling interval, with a_0, a_1, a_2, etc., being the sampled signal amplitudes at the corresponding time steps. A similar series may be written down for the signal received at B.

The correlation of the two signals may formally be expressed as

$$C_{ab}(\tau) = \int_{t_1}^{t_2} P_a(t) P_b^*(t-\tau)\,dt\,, \tag{3}$$

where $P_a(t)$ and $P_b(t)$ are both known over the time window $(t_1 \to t_2)$ of interest. In terms of the z-transform notation of Eq. (1), the normalized correlation of the two signals may be defined as

$$\begin{aligned} C_{ab}(z) &= P_a(z) P_b^*(z)/N \\ &= \left(\sum_n a_n z^n\right)\left(\sum_m b_m^*(z^m)^*\right)\Big/ N \\ &= \sum_p c_p z^p \quad (p = 0, \pm 1, \pm 2, \pm 3,\ldots)\,, \end{aligned} \tag{4}$$

where N is the normalization factor:

$$N = \left(\sum_n |a_n|^2 \sum_m |b_m|^2\right)^{1/2}. \tag{5}$$

The coefficients of Eq. (4) are then given by the following.

$$\begin{aligned} c_p &= \sum_n a_{n+p} b_n^*/N \quad (p \geqslant 0), \\ c_p &= \sum_n a_n b_{n-p}^*/N \quad (p < 0)\,. \end{aligned} \tag{6}$$

The processing of a signal (received at either A or B) through a frequency filter is formally described by a convolution integral

$$\tilde{P}_a(t) = \int_0^t P_a(\tau) R(t-\tau)\,d\tau\,, \tag{7}$$

where $R(t)$ is the impulse response of the filter, which in z-transform notation may be expressed as

$$R(z) = \sum_m r_m z^m \quad (m = 0,1,2,3,\ldots)\,. \tag{8}$$

The convolution of P_a and R is given by

$$\tilde{P}_a(z) = \sum_p \tilde{a}_p z^p \quad (p = 0,1,2,3,\ldots)\,, \tag{9}$$

where the coefficients are

$$\tilde{a}_p = \sum_n a_n r_{p-n} \quad (n = 0,1,2,3,\ldots,p)\,. \tag{10}$$

Computer algorithms based upon Eqs. (4) and (10) were developed to perform the calculations discussed next.

II. RESULTS

The formalism discussed in the previous sections was implemented to model the correlation technique for the problem shown schematically in Fig. 1. An acoustic source is

placed at a depth of 200 m in an isovelocity ocean ($c = 1500$ ms^{-1}) 5000 m deep, with a flat reflecting bottom. Two horizontally separated receivers spaced 25 m apart at a depth of 200 m are placed at a range of 5000 m from the source. Figure 1(a) shows that signals can arrive at either receiver via one of three different types of paths: a bottom-reflected (B) path, a surface-scattered/bottom-reflected (SB) path, or a bottom-reflected/surface-scattered (BS) path. Direct paths and other paths from the source to the receivers that involve multiple reflections from the ocean surface and bottom are not considered here. Figure 1(b) shows a top view of the geometry. The signals arriving at receivers A and B are sampled, filtered over the passband of 0.2- to 1.0-m wavelength, and correlated in time over a range of azimuthal angles [θ in Fig. 1(b)] from broadside ($\theta = 0$ deg) to endfire ($\theta = 90$ deg).

Scattering from the ocean surface is modeled using the facet-ensemble method applied to a long-crested wave model of the surface, as described earlier. In the ocean, wave crests can be typically 30–40 m long with a crest-to-crest distance of perhaps 10–20 m. For all of the examples considered here, the wave crests are assumed to be normal to the direction of propagation. In this regard, it is reasonable to assume that the surface is long crested across the ensonified regions for the geometries considered. The normal azimuthal orientation of the crests was selected because it provided the best case for correlation between the signals received, due to the fact that the ensonified regions are physically most similar. Any other orientation of the crests presents more physical dissimilarity and poorer signal correlation.

Figure 2 shows the magnitude of the correlation versus time delay for signals arriving via SB paths at the receivers oriented broadside and for a perfectly flat ocean surface (B and BS paths are discussed later). In this case, the paths traversed are symmetrically displaced on either side of the axis drawn from the source to the point midway between the receivers. Therefore, the two path lengths are equal, and the main correlation peak occurs at a correlation time of zero

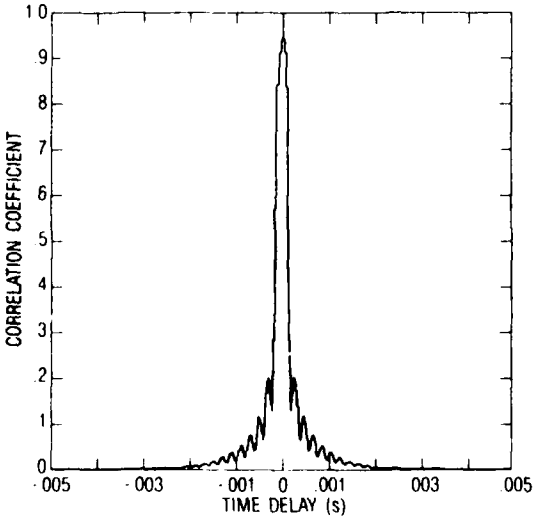

FIG. 2. Correlation versus time delay for the broadside configuration (SB ray paths) and a flat ocean surface.

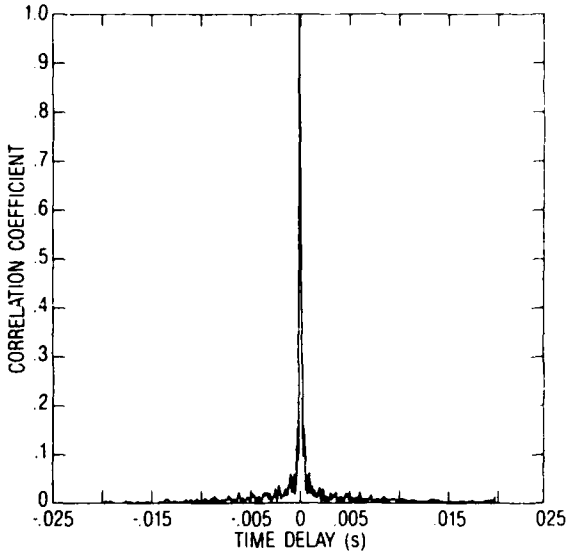

FIG. 3. Correlation curve for the broadside case ($\theta = 0$ deg, SB ray paths) for a rough ocean surface (rms waveheight = 1 m).

(i.e., at the center of the curve). Since the sea surface is perfectly flat, the sound undergoes specular reflection, just as it does from the ocean bottom. Therefore, the impulse waveform of signals arriving at the receivers is identical to that emitted by the source (in this case a narrow square pulse), but of lower intensity. After bandpass filtering, the main correlation peak, which has been normalized to have a maximum value of unity, has a shape similar to a sinc-squared function. This can be seen in Fig. 2. The shape of this correlation function is essentially determined by the Fourier transform of the bandpass filter. In Fig. 3, the correlation curve is shown for a case with an identical source/receiver configuration to that used to obtain Fig. 2. Now, however, the sea surface is no longer flat, and the surface waves are modeled in cross section and with an rms waveheight value of 1 m. Figure 4 shows a sample of the surface cross section which was derived using the wave-rider buoy data mentioned earlier.[9] The wave crests are normal to the direction of propagation and, as before, only the SB path is considered. The path lengths from the source to the two receivers are again identical, so that a main peak is observed at a correlation time of zero. However, since the sea surface is not smooth, the scattered waves have an impulse waveform re-

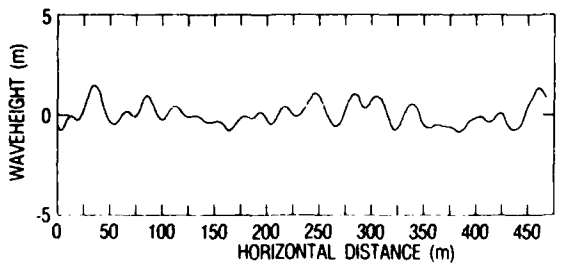

FIG. 4. Cross section of portion of ocean surface obtained from wave-rider buoy data. This surface (rms height = 1 m) was used to derive the correlation plots.

sulting from the aggregation of waves scattered from various facets on the sea surface. Since the signals are not simply specularly reflected from a flat sea surface, the impulse waveforms arriving at the receivers are radically different from the narrow spike emitted by the source. Therefore, the main correlation peak (which is again symmetric around $t = 0$ and has a maximum value of unity) no longer has the simple shape seen in Fig. 2. Instead, there is significant broadening at the base of the peak and considerable random variation stretching out both before and after the main peak. This is due to the cross correlation of delayed signals scattered from different portions of the ocean surface.

Figure 5 demonstrates the change in the correlation coefficient as the azimuthal angle of the source is increased from 0 deg (broadside) to 90 deg (endfire). Again, the wavecrests are normal to the propagation direction and only SB paths are considered. Two new features appear in this figure. First, although the curve is again normalized to unity as defined by the peak correlation coefficient calculated in the broadside case (see Fig. 3), the maximum correlation coefficient value has decreased from unity to about 0.55 due to the azimuthal rotation. The reason for this is that the signals reaching the two receivers are no longer identical, but differ because they have been scattered from different sequences of surface waves. Not only is the peak value reduced, but the symmetry of the shape of the correlation curve about the peak (observed in Figs. 2 and 3) is also lost. Second, there is a shift in the position of the correlation peak away from $t = 0$. The change in the azimuthal angle causes a corresponding change in the acoustic path lengths from the source to the receivers. One receiver moves towards the source (receiver B in Fig. 1), while the other (receiver A) moves away. The corresponding difference in the two travel times gives the shift in the peak position. In this case, its position corresponds to a time delay of 0.0075 s between the arrivals of the signals at receivers A and B. It should be noted

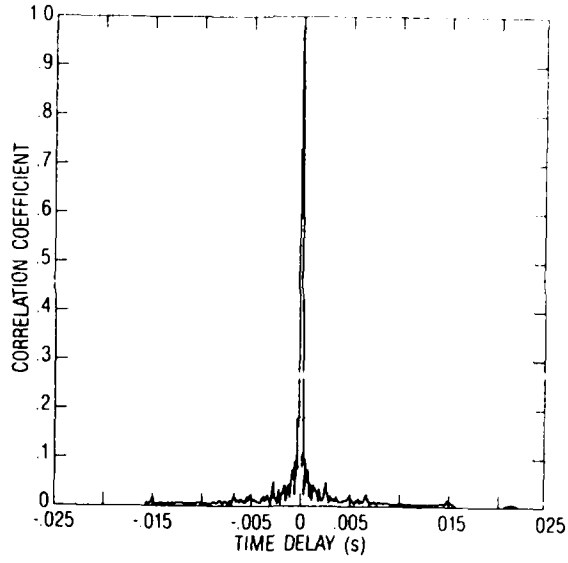

FIG. 6. Correlation curve for the broadside case ($\theta = 0$ deg) for a rough ocean surface (rms waveheight = 1 m), using BS paths only.

that even for this extreme endfire case the correlation is still good.

Figures 6 and 7 display a set of correlation curves similar to those of Figs. 3 and 5 except that now only bottom surface (BS) paths from the source to the receivers are considered, rather than SB paths. In Fig. 6, the broadside case is presented. Here, again, there exists perfect correlation: a maximum value of unity at a time delay of 0 s. This curve is similar to that of Fig. 3 for the SB case. However, marked differences between the SB and BS cases begin to appear when the azimuthal angle is increased away from broadside. This is illustrated in Fig. 7, which shows the correlation curve for an azimuthal angle of only 3 deg for the BS paths. Figure 7 should be compared with Fig. 5, which shows the corresponding curve for the SB case for endfire. Whereas, in

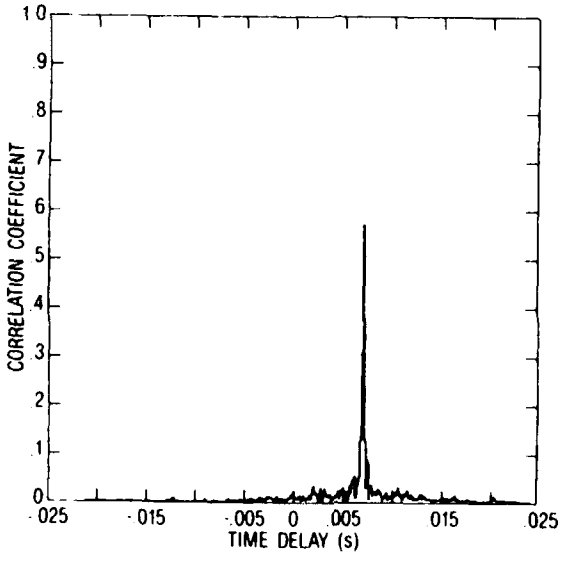

FIG. 5. Correlation curve for the endfire case ($\theta = 90$ deg, SB paths) and for a rough ocean surface (rms waveheight = 1 m).

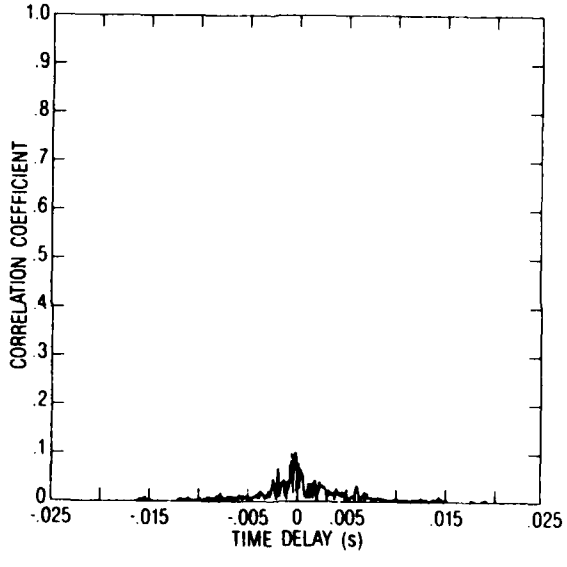

FIG. 7. Correlation curve for an azimuthal rotation of $\theta = 3$ deg from broadside, using BS paths only.

the SB case, the peak correlation coefficient drops from unity to near 0.55 for an azimuthal angle of 90 deg, in the BS case, it is approximately 0.1 for an angle of only 3 deg.

The rapid fall in the amplitude of the correlation peak in the BS case for increasing azimuth angle is best explained by examining the different paths of propagation. In the SB case, Fig. 8 shows in schematic form the paths taken by the acoustic rays as they travel from the source to the two receivers in the broadside configuration. The upper diagram shows a side view of the environmental geometry. Note that the shortest SB path between the source and either of the two receivers is taken by the ray that is specularly scattered from both the sea-surface and the sea-bottom interfaces. This is denoted the "median" path in the figure. Rays traveling along this path take the least time to pass from source to receivers via the surface and bottom. Rays that deviate from the median path take longer to pass from the source to the receivers. A time interval can be specified such that the earliest median path signals arrive at the inception of the time interval. The end of the time interval can then be used to define two "extreme" paths (see, again, Fig. 8). The points on the sea surface at which these two extreme paths reflect provide the range limits of two regions of interaction between the rays and the surface. Sound scattered from these regions may reach the detectors within the specified time period. The amount of energy arriving from outside these regions is small and can be neglected. The second of the diagrams in Fig. 8 shows the top view of the environment. Physically, scattering from the sea surface will occur from areas surrounding the points where the median paths intersect the surface. This is represented schematically in Fig. 8 by the shaded elliptical areas. The signal processing procedure used here consists of performing phase and amplitude comparisons of signals received at A and B. Since the two signals are scattered from different regions of the surface, this involves the assumption that there is some degree of phase correlation or coherence for acoustic waves scattering from different but closely adjacent regions of the sea surface. The degree of coherence is also dependent upon the wave-heights and randomness of the ocean surface. In general, however, the greater the separation between the two regions on the surface, the less correlation there will be.

In the BS case, an envelope containing the rays that carry most of the acoustic energy between source and receivers may be constructed in a similar manner to the SB case. Again, a specified time interval defines the median and extreme paths that form the ray envelope. However, in the BS case, there is an important difference. In the BS case, the rays interact with the surface *after* they are reflected from the bottom, such that the regions of ocean surface interaction are situated closer to the receivers than to the source. [This may be visualized by mentally interchanging the receiver position with the source position in Fig. 8(a) and reversing the direction of the arrowheads.] The overall size of the regions of interaction is the same as in the SB case (determined by the chosen time window, as described above), but they are much more widely separated laterally from each other due to their closer proximity to the receivers. The difference in the correlation effects between the SB and BS cases is not noticeable at broadside because, in both cases, the two signals travel to their respective receivers along effectively identical paths due to the long-crested model of the ocean surface that has been adopted. This means that perfect correlation is observed at zero time delay. However, significant differences are observed as the azimuthal angle deviates from broadside. In Fig. 9, the effect of an azimuthal rotation of the receivers on the positions of the regions of interaction is demonstrated for the SB and BS cases. It is clear from the diagram that, due to the closer proximity of these regions to receivers A and B in the BS case, they are laterally displaced with respect to each other much more in the BS than in the SB case. This means that sound scattered from these regions onto their respective receivers will have been scattered from surface

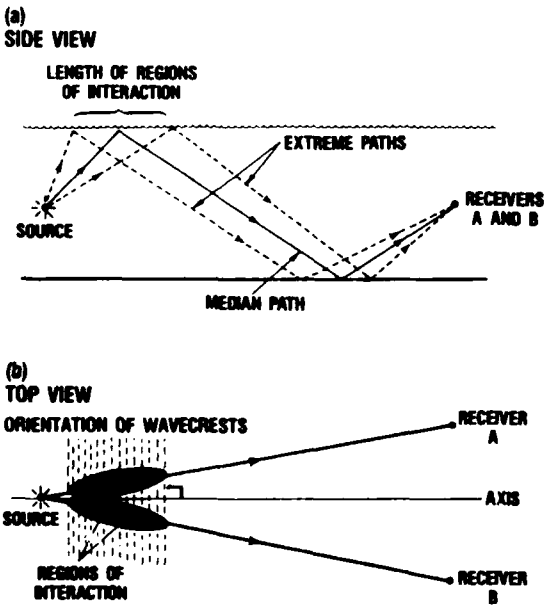

FIG. 8. Ray paths and regions of acoustic interaction with the ocean surface, for the SB case in the broadside configuration ($\theta = 0$ deg): (a) side view, (b) top view.

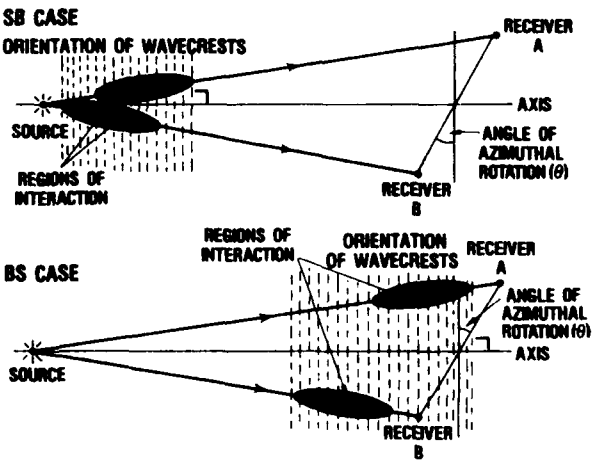

FIG. 9. Top views of the regions of acoustic interaction for the SB and BS cases after azimuthal rotation.

wave sequences, within the regions of interaction, that are less correlated physically with each other in the BS case than in the SB case. In other words, the two regions of interaction are more dissimilar in the BS case, and this gives rise to the rapid fall in correlation with increasing azimuth angle.

An effect similar to that induced by azimuthal receiver rotation is observed when the receivers are held in the broadside configuration, but the depth of one of them is slightly increased with respect to the other. In Fig. 10, the correlation curve for the SB case is shown where receiver A is held 1.5 m deeper than receiver B. Comparison of this figure with Fig. 3 shows that the effect is to decrease the amplitude of the correlation peak to 0.9, and to move its position slightly away from zero time-delay. Figure 11 shows the corresponding curve for the BS case where a dramatically decreased correlation peak amplitude is seen. The explanation is much the same as for rotation in azimuth. Dropping one receiver by 1.5 m introduces a much greater difference in the surface wave-profile encountered by the acoustic rays in the BS case than in the SB case. The signals reaching the two receivers will therefore be less correlated in the BS case.

Another interesting difference between Figs. 10 and 11 should also be noted. In Fig. 10, the correlation peak has been moved to a positive time delay from zero; whereas, in Fig. 11, it has been moved to a negative time delay. This is because, when receiver A is held 1.5 m deeper than receiver B, receiver A is reached first by the rays in the SB case, whereas it is reached second in the BS case.

All of the correlation curves shown have been formed by the comparison of two signals that are of the same type (either both SB or both BS). Figure 12 shows the correlation curve for signals arriving at receivers A and B which are comprised of rays that have traveled along both SB and B paths. It must be remembered that the time response of the bottom-reflected rays will be a short square-wave spike emitted by the source, but decreased in amplitude due to spherical spreading. This is because reflection from the bottom (which is flat and rigid) is taken here to be simply specular and introduces no incoherent scattering. In Fig. 12, the correlation curve is shown for the two receivers at the same depth in the broadside configuration and for a perfectly flat sea surface. At the position of zero time delay, a central correlation peak appears that is formed by the addition of the correlation peak for the two SB signals together with the corresponding peak for the two B signals together. In addition, two other peaks appear at time delays of ± 0.24 s. These peaks are caused by the correlation of the SB signal at

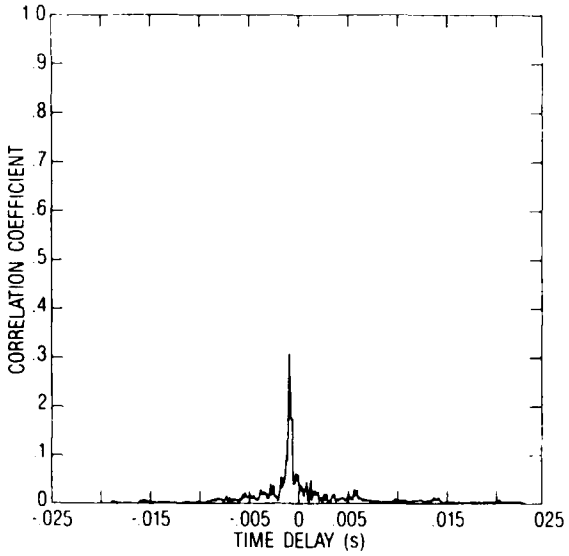

FIG. 11. Correlation curve for the broadside case ($\theta = 0$ deg, BS paths), for a rough ocean surface (rms waveheight = 1 m), and with one receiver held 1.5 m deeper than the other.

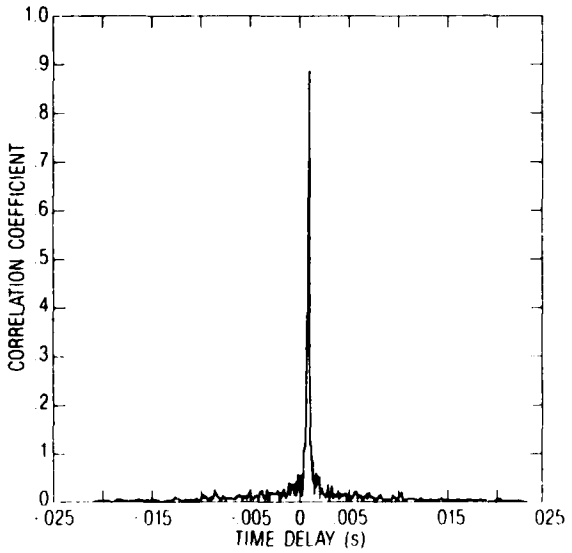

FIG. 10. Correlation for the broadside case (SB paths) for a rough ocean surface (rms waveheight = 1 m), and with one receiver held 1.5 m deeper than the other.

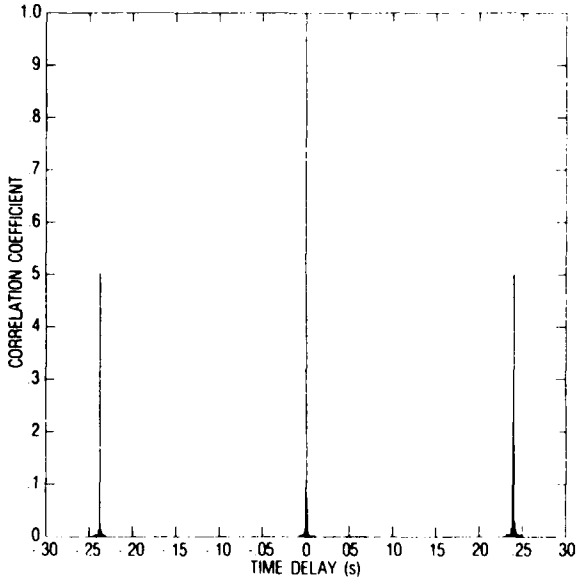

FIG. 12. Correlation for the broadside case ($\theta = 0$ deg) with a flat ocean surface. The cross correlation is shown between both SB and B path signals. The high central peak is due to SB–SB and B–B cross correlations. The two smaller side lobes are due to SB–B and B–SB cross correlations.

receiver A with the B signal at receiver B, and vice versa. The main peak has a normalized value of 1 and the side peaks have values of 0.5 each. These are the values one would expect for a perfectly flat ocean surface and ocean bottom. For the same configuration of source and receiver positions, but with a rough sea surface with waves of rms height 1 m, the level of the side peaks drops from 0.5 to 0.21. There is no appreciable fall in the level of the central peak (cf. Figs. 2 and 3). For the endfire configuration (with rough surface), which is the worst geometrically, the amplitude of the central peak falls to 0.63 but is still clearly distinguishable from the sidelobes, which have an average value $\cong 0.3$. Also, even though the central peak is now formed by the addition of the correlation peak for the two SB signals together with the peak for the two B signals together, these two peaks do not separate in the endfire configuration. Therefore, information contained in the main peak should be usable.

III. CONCLUSIONS

A z-transform technique has been presented and used in conjunction with the time-domain facet-ensemble method to compute coherence versus time delay for two receivers. It showed that, for a rough ocean surface and a flat rigid bottom, signals arriving via SB paths possess greater coherence than signals arriving via BS paths. The dissimilarity between the two scattering regions on the ocean surface for the two receivers is greater in the case of the BS paths than the SB paths. This implies that, for the purpose of correlating the signals arriving at the two receivers in the presence of ocean surface roughness (with a flat rigid bottom), it is more advantageous to use bottom arriving energy than surface arriving energy. This remains true when signals arriving via SB and B paths are superposed.

ACKNOWLEDGMENTS

The authors wish to acknowledge several helpful discussions with Professor C. S. Clay concerning the z-transform technique, and would like to thank Dr. Joe W. Posey, Peter D. Herstein, and the reviewer for their comments on the manuscript. This work was supported by NORDA.

[1] W. A. Kinney, C. S. Clay, and G. S. Sandness, "Scattering from a corrugated surface: Comparison between experiment, Helmholtz–Kirchhoff theory and the facet-ensemble method " (accepted for publication in J. Acoust. Soc. Am.).

[2] C. S. Clay and W. A. Kinney, "Numerical computation of time-domain reflections from wedges and reflections from facets," J. Acoust. Soc. Am. **83**, 2126–2133 (1988).

[3] B. E. Parkins, "Coherence of acoustic signals reradiated from the time-varying surface of the ocean," J. Acoust. Soc. Am. **45**, 119–123 (1968).

[4] J. F. McDonald, F. B. Tuteur, and J. G. Zornig, "Spatial interfrequency correlation effects in a surface-scatter channel," J. Acoust. Soc. Am. **59**, 1284–1293 (1976).

[5] M. H. Brill, X. Zabal, and S. L. Adams, "Time spread of acoustic signals reflecting from a fixed rough boundary," J. Acoust. Soc. Am. **75**, 1062–1070 (1984).

[6] X. Zabal, M. H. Brill, and J. L. Collins, "Frequency and angle spreads of acoustic signals reflecting from a fixed rough boundary," J. Acoust. Soc. Am. **79**, 673–680 (1986).

[7] W. A. Kinney and C. S. Clay, "The spatial coherence of sound scattered from a wind-driven surface: Comparison between experiment, Eckart theory, and the facet-ensemble method," J. Acoust. Soc. Am **75**, 145–148 (1984).

[8] W. A. Kinney and J. G. Zornig, "Modeling the azimuthal dependence of bistatic surface scattering," J. Acoust. Soc. Am. **77**, 1403–1408 (1985).

[9] W. I. Roderick, NUSC (private communication).

[10] A. V. Oppenheim and R. W. Schafer, *Digital Signal Processing* (Prentice-Hall, Englewood Cliffs, NJ, 1975), Chap. 2.